

SHOCK DYNAMICS IN RELATIVISTIC JETS

J. Cantó¹, S. Lizano^{2*}, M. Fernández-López^{1,3}, R. F. González²,
and A. Hernández-Gómez^{1,4}

¹*Instituto de Astronomía, UNAM, Apdo. Postal 70-264, 04510 México D. F., México*

²*Centro de Radioastronomía y Astrofísica, UNAM, Apdo. Postal 3-72, Morelia, Michoacán 58089, México*

³*Department of Astronomy, University of Illinois, 1002 West Green Street, Urbana, IL 61801, USA*

⁴*Instituto de Ciencias Físicas, UNAM, Apdo. Postal 48-3, Cuernavaca, Morelos 62210, México*

January 26, 2013

ABSTRACT

We present a formalism of the dynamics of internal shocks in relativistic jets where the source has a time-dependent injection velocity and mass-loss rate. The variation of the injection velocity produces a two-shock wave structure, the working surface, that moves along the jet. This new formalism takes into account the fact that momentum conservation is not valid for relativistic flows where the relativistic mass lost by radiation must be taken into account, in contrast to the classic regime. We find analytic solutions for the working surface velocity and radiated energy for the particular case of a step function variability of the injection parameters. We model two cases: a pulse of fast material and a pulse of slow material (with respect to the mean flow). Applying these models to gamma ray burst light curves, one can determine the ratio of the Lorentz factors γ_2/γ_1 and the ratio of the mass-loss rates \dot{m}_2/\dot{m}_1 of the upstream and downstream flows. As an example, we apply this model to the sources GRB 080413B and GRB 070318 and find the values of these ratios. Assuming a Lorentz factor $\gamma_1 = 100$, we further estimate jet mass-loss rates between $\dot{m}_1 \sim 10^{-5} - 1 M_\odot \text{ yr}^{-1}$. We also calculate the fraction of the injected mass lost by radiation. For GRB 070318 this fraction is $\sim 7\%$. In contrast, for GRB 080413B this fraction is larger than 50%; in this case radiation losses clearly affect the dynamics of the internal shocks.

Key words: hydrodynamics – shock waves – relativity – galaxies: jets – gamma-ray: bursts

1 INTRODUCTION

Collimated outflows (with jet-like geometry) moving at relativistic speeds are characteristic of active galactic nuclei. It is commonly accepted that an extragalactic jet is produced in the neighborhood of a massive black hole in the center of an active galaxy (e.g. Rees 1984; Istomin 2010). These relativistic jets are subject to the development of shock waves. Rees (1978) proposed that the observed knots in the extragalactic jet M87 correspond to the locations of internal shocks which arise owing to variations in the outflow velocity of a beam generated in the nucleus. Later, Rees & Mészáros (1994) pointed out that fluctuations of the Lorentz factor around its mean value in a relativistic outflow, that give rise to internal shocks, can dissipate a substantial fraction of the outflow energy into non-thermal radiation. They proposed that this mechanism is operating in the so-called gamma-ray bursts (GRBs).

Several authors have studied internal shocks in ultra-relativistic outflows to explain the observed variability of GRBs (e.g., Mochkovitch, Maitia & Marques 1995; Kobayashi, Piran & Sari 1997; Daigne & Mochkovitch 1998; 2000). In these models the flow is represented by a succession of shells with different values of the Lorentz factor. This models reproduce the burst profiles and their short-time scale variability. Kobayashi et al. pointed out that variations of the relativistic flow velocity are strongly correlated with the temporal variations observed in the GRBs. Daigne & Mochkovitch (1998) studied the detailed radiation processes to calculate the fraction of the kinetic energy dissipated in the shocks that can be emitted in the form of gamma rays and obtained that the total efficiency is of the order of only a few percent. In addition, Spada et al. (2001) proposed that the internal shock scenario can also be used for blazars. For comprehensive reviews of the physical processes and observations of GRBs see, e.g., Mészáros (2002); Piran (2004); and Gehrels et al. (2009).

Using mass and momentum conservation, Cantó et al. (2000) solved the dynamics of internal shocks of non rela-

* E-mail: s.lizano@crya.unam.mx

tivistic jets with time dependent injection velocity and mass-loss rate. Mendoza et al. (2009) used this momentum conserving formalism in the case of relativistic jets and compared with observed light curves of GRBs assuming a sinusoidal velocity variation. However, momentum is not conserved in relativistic flows because radiative losses change the relativistic mass since the Lorentz factor decreases when energy is radiated away. In this paper we present a new formalism that describes the dynamics of internal shocks in a relativistic jet taking into account the momentum change by radiation. In particular, we study the dynamics of internal shocks for the case where the injection velocity and mass-loss rate are both step functions of time, when a fast wind reaches a slower flow. For this type of variability, we find analytic solutions for the dynamical evolution and luminosity of the shocks, which are implicit functions of time.

The organization of the paper is as follows. In §2 we discuss the relevant relativistic equations. In §3 we present the model, and investigate the dynamical evolution of the internal WS. The luminosities predicted by our model from relativistic jets are given in §4. A comparison between our analytic solutions and observations of extragalactic gamma ray bursts are presented in §5. In §6 we evaluate the mass lost by radiation in the WS. Finally, in §7 we summarize our conclusions.

2 RELATIVISTIC EQUATIONS FOR INTERNAL SHOCKS

For a free-streaming flow, the non-dimensional velocity at a distance x from the source, at time t measured at the source reference frame, is given by

$$\beta(x, t) = \beta(0, \tau) = \frac{x}{c(t - \tau)}, \quad (1)$$

where the injection point is at $x = 0$, and τ is the time at which the flow was ejected, and, as usual, $\beta = v/c$, where v and c are the speeds of the flow and of light, respectively. If the flow velocity at the injection point increases, the fast material will reach the slower material and form a working surface (WS) bounded by two shock fronts (Raga et al. 1990). These WS structures are the so-called “internal shocks”. Figure 1 shows a schematic diagram of a WS formed when a fast upstream material with velocity β_2 reaches a slower downstream material with velocity β_1 . The WS moves with velocity β_{ws} intermediate between β_1 and β_2 .

The internal WS forms at the distance x_i from the source given by

$$\frac{x_i}{c} = \left[\frac{\beta(\tau)^2}{d\beta(\tau)/d\tau} \right]_{\min}, \quad (2)$$

where we wrote for simplicity, $\beta(\tau) = \beta(0, \tau)$, and the minimum is taken over the time interval where the velocity increases. The WS is formed at time t_i from the material ejected at time τ_i , both values given by equation (2)¹. Then, one can obtain the time, t_i , at which the WS is formed from equation (1).

Consider a relativistic jet with time dependent injection velocity, $\beta(\tau)$, and mass-loss rate, $\dot{m}(\tau)$. As discussed

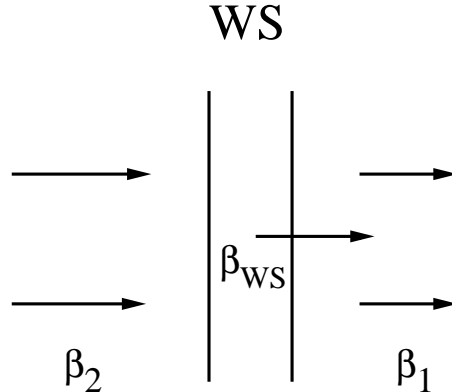


Figure 1. Schematic diagram showing a working surface formed by the interaction between two relativistic flows. The upstream and downstream flow velocities are β_2 and β_1 (with $\beta_2 > \beta_1$), respectively. The working surface moves with an intermediate velocity β_{ws} .

above, a WS is formed when fast material overtakes slow material. This WS travels downstream the jet flow with a velocity $\beta_{ws}(t)$, where the time t is measured in the source reference frame. The slow and the fast material just entering the WS at time t were ejected at times τ_1 and τ_2 , respectively, with corresponding downstream and upstream velocities $\beta_1 = \beta(\tau_1)$ and $\beta_2 = \beta(\tau_2)$, and mass-loss rates, $\dot{m}_1 = \dot{m}(\tau_1)$ and $\dot{m}_2 = \dot{m}(\tau_2)$. The time dependence of the velocities and mass-loss rates is given through the time dependences $\tau_1(t)$, and $\tau_2(t)$.

In Appendix A we discuss a simple example of the inelastic collision of 3 relativistic particles that radiate energy after they collide. This example shows that the momentum of the final particle is not conserved because its relativistic mass changes when energy is radiated away. Therefore, we introduce below the energy and momentum equations that take into account the energy lost by radiation.

The total energy dissipated by the flow interaction $E(t)$ is given by the difference between the total energy injected into the WS and the energy carried by the WS at the instant t ²,

$$\frac{E(t)}{c^2} = \int_{\tau_1}^{\tau_2} \dot{m}(\tau)\gamma(\tau)d\tau - m_{ws}(t)\gamma_{ws}(t), \quad (3)$$

where $\gamma_{ws}(t) = 1/\sqrt{1 - \beta_{ws}(t)^2}$, and the rest mass injected into the WS is

$$m_{ws}(t) = \int_{\tau_1}^{\tau_2} \dot{m}(\tau)d\tau. \quad (4)$$

We assume that dissipated energy $E(t)$ is completely radiated away (see eq. [A9]); none of this energy is stored in internal degrees of freedom. Therefore, the luminosity (the radiated energy per unit time in the WS) is given by the time derivative $L_r(t) = dE(t)/dt$. Then, the dynamics of the WS is described by the energy equation,

$$\frac{d}{dt} (m_{ws}(t)\gamma_{ws}(t)) = \frac{d}{dt} \int_{\tau_1}^{\tau_2} \dot{m}(\tau)\gamma(\tau)d\tau - \frac{L_r(t)}{c^2}, \quad (5)$$

¹ First, τ_i is obtained by minimizing the RHS of this equation.

² For simplicity, the internal energy of the particles that enter the WS is ignored.

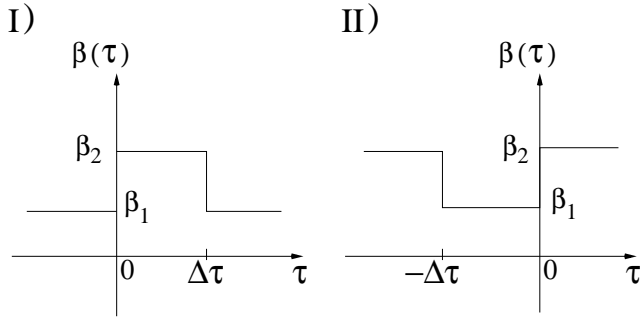


Figure 2. Injection velocity β as function of time τ : I) The initial velocity β_1 suddenly increases to β_2 at a time $\tau = 0$, for a finite time interval, $\Delta\tau$, and then instantly returns back to its original value. II) The initial velocity β_2 instantly decreases to β_1 at a time $\tau = -\Delta\tau$, and at $\tau = 0$, the faster flow starts to be injected again.

obtained from the derivative of equation (3), and the momentum equation is given by

$$\frac{d}{dt}(m_{\text{ws}}(t)\gamma_{\text{ws}}(t)\beta_{\text{ws}}(t)) = \frac{d}{dt} \int_{\tau_1}^{\tau_2} \dot{m}(\tau)\gamma(\tau)\beta(\tau)d\tau - \frac{L_r(t)}{c^2}\beta_{\text{ws}}(t), \quad (6)$$

where the last term in the RHS is the momentum change due to the relativistic mass lost by radiation. Combining equations (5) and (6) one obtains the equation for the velocity of the WS,

$$\begin{aligned} m_{\text{ws}}(t)\gamma_{\text{ws}}(t)\frac{d\beta_{\text{ws}}}{dt} &= \frac{d}{dt} \int_{\tau_1}^{\tau_2} \dot{m}(\tau)\gamma(\tau)\beta(\tau)d\tau \\ &\quad - \beta_{\text{ws}}(t)\frac{d}{dt} \int_{\tau_1}^{\tau_2} \dot{m}(\tau)\gamma(\tau)d\tau \\ &= \dot{m}(\tau_2)\gamma(\tau_2) [\beta(\tau_2) - \beta_{\text{ws}}(t)] \frac{d\tau_2}{dt} \\ &\quad - \dot{m}(\tau_1)\gamma(\tau_1) [\beta(\tau_1) - \beta_{\text{ws}}(t)] \frac{d\tau_1}{dt}, \end{aligned} \quad (7)$$

that does not depend explicitly on the radiated energy, L_r .

Given a time variability of the functions $\beta(\tau)$ and $\dot{m}(\tau)$, one can find the WS velocity, $\beta_{\text{ws}}(t)$, from equation (7) together with equation (1), the latter giving the relation between $\tau_{1,2}$ and t . We will show below how these equations can be solved analytically for the case of step function variability of the injection parameters.

3 STEP FUNCTION VARIABILITY OF THE INJECTION PARAMETERS

Consider a step function variability for the injection velocity and mass-loss rate such that, for $\tau < 0$, a slow flow has $\beta = \beta_1$, and $\dot{m} = \dot{m}_1$; and for $\tau \geq 0$, a fast flow has $\beta = \beta_2$ and $\dot{m} = \dot{m}_2$. Figure 2 shows two cases: I) when fast material is injected at $\tau > 0$ for a finite time, $\Delta\tau$; and II) when slow material is injected at $\tau < 0$, for a finite time interval, $\Delta\tau$. In both cases, when the fast flow reaches the slow flow, the WS is formed instantaneously at the injection point: $x = 0$, $t = 0$, and $\tau = 0$.

As we will show below, the dynamical evolution of the WS goes through 2 stages. In the first stage, the WS is fed by

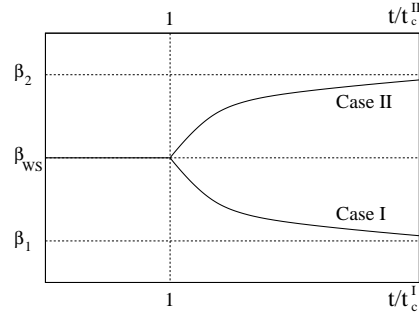


Figure 3. Qualitative behavior of the WS velocity as a function of normalized time $t/t_c^{I,II}$, for Case I and Case II, respectively. See text for description of this figure.

both the slow and fast flows and it moves at a constant velocity, intermediate between the fast and slow speeds. The second stage begins when one of the flows has been completely incorporated into the WS; then, the WS accelerates or decelerates depending on which flow (fast or slow) continues to feed the remaining shock. Asymptotically in time, the speed of the WS in the second stage tends to the velocity of the remaining flow.

Figure 3 shows the qualitative behavior of the WS velocity as a function of normalized time for Case I (pulse of fast material) and Case II (pulse of slow material). In Case I, the time is normalized to the critical time t_c^I (eq. [14]). In Case II, the time is normalized to the critical time t_c^{II} (eq. [26]). In both cases, the constant velocity phase ends when $t/t_c^{I,II} = 1$.

Consider the material at time t that enters the WS, located at the position $x_{\text{ws}}(t)$, through both shocks. The slow and fast material were ejected at times τ_1 and τ_2 , respectively, such that, according to equation (1)

$$\tilde{\tau}_{1,2} = \tilde{t} - \frac{\tilde{x}_{\text{ws}}}{\beta_{1,2}} \quad \text{and} \quad \frac{d\tilde{\tau}_{1,2}}{d\tilde{t}} = 1 - \frac{\beta_{\text{ws}}}{\beta_{1,2}}, \quad (8)$$

where $\tilde{\tau}_{1,2} = \tau_{1,2}/\Delta\tau$, $\tilde{t} = t/\Delta\tau$, and $\tilde{x}_{\text{ws}} = x_{\text{ws}}/(c\Delta\tau)$.

Now, for a step function variability, the rest mass of the WS, given by equation (4), is

$$\begin{aligned} m_{\text{ws}}(t) &= \int_{\tau_1}^0 \dot{m}_1(\tau)d\tau + \int_0^{\tau_2} \dot{m}_2(\tau)d\tau \\ &= -\dot{m}_1\tau_1(t) + \dot{m}_2\tau_2(t). \end{aligned} \quad (9)$$

Note that $\tau_1 < 0$ and $\tau_2 > 0$, and for now on, for simplicity, we will drop the t dependence of the functions.

The velocity of the WS is obtained from equation (7)

$$m_{\text{ws}}\gamma_{\text{ws}}\frac{d\beta_{\text{ws}}}{dt} = \dot{m}_2\gamma_2\frac{(\beta_2 - \beta_{\text{ws}})^2}{\beta_2} - \dot{m}_1\gamma_1\frac{(\beta_1 - \beta_{\text{ws}})^2}{\beta_1}, \quad (10)$$

where we used equation (8). This equation has the constant velocity, $\beta_{\text{ws}0}$, solution³, such that $d\beta_{\text{ws}0}/dt = 0$, then,

$$\lambda(\beta_2 - \beta_{\text{ws}0}) = \pm(\beta_{\text{ws}0} - \beta_1), \quad (11)$$

with

$$\lambda = \sqrt{\frac{\dot{m}_2\gamma_2\beta_1}{\dot{m}_1\gamma_1\beta_2}} = \sqrt{\frac{br}{a}}, \quad (12)$$

³ This solution exists because at $t = 0$, the initial condition $\beta_{\text{ws}0}$ makes the RHS of the equation equal zero, since $m_{\text{ws}}(0) = 0$.

where we defined the velocity ratio $a = \beta_2/\beta_1$, the mass-loss rate ratio $b = \dot{m}_2/\dot{m}_1$, and gamma ratio $r = \gamma_2/\gamma_1$. The correct solution corresponds to the + sign⁴, with the ordering $\beta_1 < \beta_{ws} < \beta_2$, where the constant WS velocity is given by

$$\beta_{ws0} = \frac{\lambda\beta_2 + \beta_1}{\lambda + 1}, \quad \text{and} \quad \gamma_{ws0} = \frac{\lambda + 1}{\sqrt{(\lambda/\gamma_2)^2 + 2\lambda(1 - \beta_1\beta_2) + 1/\gamma_1^2}}. \quad (13)$$

This velocity corresponds to the first stage of the evolution of the WS, when it is fed (and bounded) by two shocks.

Now we will discuss the evolution of the WS in the second stage of the two different cases I and II shown in Figure 2. Even though the formalism is the same, the resulting equations are different for each case. Thus, for clarity, we separate them in the next two subsections.

3.1 Case I: Decelerating WS

The constant velocity phase ends when $\tau_2 = \Delta\tau$, i.e., when the fast material is completely incorporated into the WS. This happens at a critical time obtained by substituting the position of the WS, $\tilde{x}_{ws0} = \beta_{ws0}\tilde{t}$, into equation (8),

$$\tilde{t}_c^I = \frac{a(\lambda + 1)}{a - 1}, \quad (14)$$

which corresponds to ejection time

$$\tilde{\tau}_{1,c} = \tilde{t}_c^I \left(1 - \frac{\beta_{ws0}}{\beta_1} \right) = -a\lambda. \quad (15)$$

In this second stage, $\tilde{t} > \tilde{t}_c^I$, the first term of equation (7) is 0 because $d\tau_2/dt = 0$. Furthermore, substituting $\tau_2 = \Delta\tau$ in equation (9), the rest mass of the WS is

$$m_{ws} = \dot{m}_2\Delta\tau - \dot{m}_1\tau_1 = \dot{m}_1\Delta\tau(b - \tilde{\tau}_1). \quad (16)$$

Collecting these results we write the WS velocity in equation (7) as function of $\tilde{\tau}_1$ as

$$\frac{d\beta_{ws}}{d\tilde{\tau}_1} = \frac{\gamma_1(\beta_{ws} - \beta_1)}{\gamma_{ws}(b - \tilde{\tau}_1)}. \quad (17)$$

For $\beta_{ws} \neq \beta_1$, this equation⁵ can be integrated by separation of variables as

$$\frac{2(\gamma_1 - \beta_{ws}\beta_1\gamma_1 + 1/\gamma_{ws})}{(\beta_{ws} - \beta_1)} = C^I(b - \tilde{\tau}_1), \quad (18)$$

that is a quadratic equation for $\beta_{ws}(\tilde{\tau}_1)$, and has the solution

$$\beta_{ws}(\tilde{\tau}_1) = \frac{\beta_1\mathcal{T}^2 + 4\mathcal{T} + 4\beta_1}{\mathcal{T}^2 + 4\beta_1\mathcal{T} + 4} \quad \text{and} \quad \gamma_{ws}(\tilde{\tau}_1) = \gamma_1 \left(\frac{\mathcal{T}^2 + 4\beta_1\mathcal{T} + 4}{\mathcal{T}^2 - 4} \right), \quad (19)$$

where we defined the time function

$$\mathcal{T}(\tilde{\tau}_1) = \frac{C^I(b - \tilde{\tau}_1)}{\gamma_1}, \quad (20)$$

⁴ The - sign in equation (11) is unphysical because, in this solution, $\beta_{ws0} < \beta_1$, that implies that there is no downstream shock.

⁵ Equation 17 has a constant velocity solution, $\beta_{ws} = \beta_1$, that is trivial because there is no shock.

that is an increasing function of $|\tilde{\tau}_1|$. From equation (18) one can show that $\mathcal{T}(\tilde{\tau}_1) > 2$. The constant C^I is obtained by matching the solution $\beta_{ws}(\tilde{\tau}_{1,c}) = \beta_{ws0}$, where $\tilde{\tau}_{1,c}$ is given by equation (15); thus, from equation (18) one gets

$$C^I = \frac{2(\gamma_1 - \beta_{ws0}\beta_1\gamma_1 + 1/\gamma_{ws0})}{(b + a\lambda)(\beta_{ws0} - \beta_1)}. \quad (21)$$

To find a relation between $\tilde{\tau}_1$ and \tilde{t} , we take the derivative of the time function \mathcal{T} (eq. [20]),

$$\frac{d\mathcal{T}}{d\tilde{t}} = -\frac{C^I}{\gamma_1} \frac{d\tilde{\tau}_1}{d\tilde{t}} = \frac{4C^I}{\beta_1\gamma_1^3} \frac{\mathcal{T}}{(\mathcal{T}^2 + 4\beta_1\mathcal{T} + 4)}, \quad (22)$$

where we used equations (8) and (19). Again, by separation of variables, this equation can be integrated as

$$\frac{\mathcal{T}^2}{2} + 4\beta_1\mathcal{T} + 4 \ln \mathcal{T} = \frac{4C^I}{\beta_1\gamma_1^3} \tilde{t} + D^I, \quad (23)$$

where the constant D^I is obtained evaluating this expression at \tilde{t}_c^I and $\tilde{\tau}_{1,c}$, and is given by,

$$D^I = \frac{\mathcal{T}_c^2}{2} + 4\beta_1\mathcal{T}_c + 4 \ln \mathcal{T}_c - \frac{4C^I}{\beta_1\gamma_1^3} \frac{a(\lambda + 1)}{(a - 1)}, \quad (24)$$

where the critical time function is

$$\mathcal{T}_c = \mathcal{T}(\tilde{\tau}_{1,c}) = C^I \frac{(b + a\lambda)}{\gamma_1}. \quad (25)$$

Therefore, given $\tilde{\tau}_1$ one can evaluate the time function \mathcal{T} to obtain $\beta_{ws}(\tilde{\tau}_1)$ from equations (19) and (20), and one can obtain the WS velocity as a function of time \tilde{t} , $\beta_{ws}(\tilde{t})$, in a tabular form, using equation (23). Finally, the position of the WS, $x_{ws}(\tilde{t})$, is given by equation (8).

3.2 Case II: Accelerating WS

In this case, the constant velocity phase ends when $\tau_1 = -\Delta\tau$, i.e., when the slow material is completely incorporated into the WS. From equation (8), the critical time is

$$\tilde{t}_c^{II} = \frac{(\lambda + 1)}{\lambda(a - 1)}, \quad (26)$$

corresponding to the ejection time

$$\tilde{\tau}_{2,c} = \tilde{t}_c^{II} \left(1 - \frac{\beta_{ws0}}{\beta_2} \right) = \frac{1}{a\lambda}. \quad (27)$$

For $\tilde{t} > \tilde{t}_c^{II}$, one has $d\tau_1/dt = 0$. Also, from equation (9), the rest mass is

$$m_{ws} = \dot{m}_2\tau_2 + \dot{m}_1\Delta\tau = \dot{m}_1\Delta\tau(b\tilde{\tau}_2 + 1). \quad (28)$$

Then, we write the WS velocity in equation (7) as function of $\tilde{\tau}_2$ as

$$\frac{d\beta_{ws}}{d\tilde{\tau}_2} = \frac{\gamma_2b(\beta_2 - \beta_{ws})}{\gamma_{ws}(b\tilde{\tau}_2 + 1)}. \quad (29)$$

For $\beta_{ws} \neq \beta_2$, this equation⁶ can be integrated by separation of variables as

$$\frac{2(\gamma_2 - \beta_{ws}\beta_2\gamma_2 + 1/\gamma_{ws})}{(\beta_2 - \beta_{ws})} = C^{II}(b\tilde{\tau}_2 + 1), \quad (30)$$

⁶ Equation 29 has a constant velocity solution, $\beta_{ws} = \beta_2$, which is trivial because there is no shock.

which is a quadratic equation for $\beta_{ws}(\tilde{\tau}_2)$, and has the solution

$$\beta_{ws}(\tilde{\tau}_2) = \frac{\beta_2 \mathcal{T}^2 - 4\mathcal{T} + 4\beta_2}{\mathcal{T}^2 - 4\beta_2 \mathcal{T} + 4}, \quad \text{and}$$

$$\gamma_{ws}(\tilde{\tau}_2) = \gamma_2 \left(\frac{\mathcal{T}^2 - 4\beta_2 \mathcal{T} + 4}{\mathcal{T}^2 - 4} \right), \quad (31)$$

where the time function is

$$\mathcal{T}(\tilde{\tau}_2) = \frac{C^{II}(b\tilde{\tau}_2 + 1)}{\gamma_2}, \quad (32)$$

that is an increasing function of $\tilde{\tau}_2$. As in the previous case, one can show that $\mathcal{T}(\tilde{\tau}_2) > 2$. The constant C^{II} is obtained by matching the solution $\beta_{ws}(\tilde{\tau}_{2,c}) = \beta_{ws0}$, where $\tilde{\tau}_{2,c}$ is given by equation (27). Substituting these results into equation (30) one gets

$$C^{II} = \frac{2a\lambda(\gamma_2 - \beta_{ws0}\beta_2\gamma_2 + 1/\gamma_{ws0})}{(b+a\lambda)(\beta_2 - \beta_{ws0})}. \quad (33)$$

We take the derivative of the time function \mathcal{T} (eq. [32]),

$$\frac{d\mathcal{T}}{d\tilde{\tau}_2} = \frac{C^{II}b}{\gamma_2} \frac{d\tilde{\tau}_2}{d\tilde{\tau}_2} = \frac{4C^{II}}{\beta_2\gamma_2^3} \frac{\mathcal{T}}{(\mathcal{T}^2 - 4\beta_2\mathcal{T} + 4)}, \quad (34)$$

where we used equations (8) and (31). By separation of variables, this equation can be integrated as

$$\frac{\mathcal{T}^2}{2} - 4\beta_2\mathcal{T} + 4 \ln \mathcal{T} = \frac{4C^{II}}{\beta_2\gamma_2^3} \tilde{t} + D^{II}, \quad (35)$$

where the constant D^{II} is obtained evaluating this expression at \tilde{t}_c^{II} and $\tilde{\tau}_{2,c}$, and is given by,

$$D^{II} = \frac{\mathcal{T}_c^2}{2} - 4\beta_2\mathcal{T}_c + 4 \ln \mathcal{T}_c - \frac{4C^{II}}{\beta_2\gamma_2^3} \frac{(\lambda + 1)}{\lambda(a-1)}, \quad (36)$$

where the critical time function is

$$\mathcal{T}_c = \mathcal{T}(\tilde{\tau}_{2,c}) = C^{II} \frac{(b+a\lambda)}{a\lambda\gamma_2}. \quad (37)$$

Using equations (8), (31), (32), and (35) one can proceed as in Case I to obtain $\beta_{ws}(\tilde{t})$ and $x_{ws}(\tilde{t})$ as functions of t in a tabular form.

4 LUMINOSITIES

Using a step function variability of the injection parameters in equation (5), the luminosity L_r of the WS is given by

$$\begin{aligned} \frac{L_r(\tilde{t})}{c^2} &= \dot{m}_2\gamma_2 \frac{d\tilde{\tau}_2}{d\tilde{t}} - \dot{m}_1\gamma_1 \frac{d\tilde{\tau}_1}{d\tilde{t}} \\ &+ \left(\dot{m}_1 \frac{d\tilde{\tau}_1}{d\tilde{t}} - \dot{m}_2 \frac{d\tilde{\tau}_2}{d\tilde{t}} \right) \gamma_{ws} - \frac{m_{ws}}{\Delta\tau} \frac{d\gamma_{ws}}{d\tilde{t}} \\ &= \dot{m}_2(\gamma_2 - \gamma_{ws}) \frac{d\tilde{\tau}_2}{d\tilde{t}} + \dot{m}_1(\gamma_{ws} - \gamma_1) \frac{d\tilde{\tau}_1}{d\tilde{t}} \\ &- \frac{m_{ws}}{\Delta\tau} \frac{d\gamma_{ws}}{d\tilde{t}}. \end{aligned} \quad (38)$$

where we have used equation (9) for the rest mass m_{ws} .

Only a fraction of the energy radiated in internal shocks will be emitted as gamma rays; this fraction is low, $\epsilon \sim 0.01$ (e.g., Daigne & Mochkovitch 1998). Here we will assume that a constant fraction ϵ of the luminosity will go into gamma

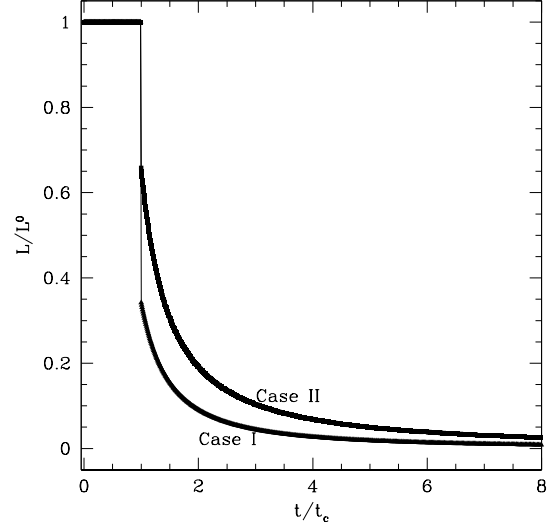


Figure 4. Normalized luminosity L/L^0 , as function of the normalized time t/t_c for Case I and Case II. For these models, we assumed $\gamma_1 = 100$ and $\gamma_2 = 200$. We also assumed $\lambda = 1$, thus, the critical times are the same for both cases.

ray radiation, $L_{GRB} = \epsilon L_r(t)$, and express this GRB luminosity in non dimensional form as

$$\begin{aligned} \tilde{L} &= \frac{L_{GRB}}{\epsilon c^2 \gamma_1 \dot{m}_1} \\ &= a\lambda^2 \frac{(\gamma_2 - \gamma_{ws})}{\gamma_2} \frac{d\tilde{\tau}_2}{d\tilde{t}} + \frac{(\gamma_{ws} - \gamma_1)}{\gamma_1} \frac{d\tilde{\tau}_1}{d\tilde{t}} \\ &- \frac{m_{ws}}{\dot{m}_1 \gamma_1 \Delta\tau} \frac{d\gamma_{ws}}{d\tilde{t}}. \end{aligned} \quad (39)$$

In the constant velocity phase, $\tilde{t} < \tilde{t}_c^{II}$, the luminosity is given by

$$\begin{aligned} \tilde{L}^0 &= \lambda^2 \frac{(\gamma_2 - \gamma_{ws0})}{\gamma_2} \left(a - \frac{\beta_{ws0}}{\beta_1} \right) \\ &- \frac{(\gamma_{ws0} - \gamma_1)}{\gamma_1} \left(\frac{\beta_{ws0}}{\beta_1} - 1 \right) \\ &= \left(\frac{\beta_{ws0}}{\beta_1} - 1 \right) \left[\lambda \frac{(\gamma_2 - \gamma_{ws0})}{\gamma_2} - \frac{(\gamma_{ws0} - \gamma_1)}{\gamma_1} \right], \end{aligned} \quad (40)$$

where we substituted $d\tilde{\tau}_1/d\tilde{t} = 1 - \beta_{ws}/\beta_1$ and $d\tilde{\tau}_2/d\tilde{t} = 1 - \beta_{ws}/\beta_2$ from equation (8).

As mentioned in §3.1, in Case I, once all the fast material has been completely incorporated into the working surface, it is decelerated by the slow downstream flow. This second stage starts at a time \tilde{t}_c^I given by equation (14). For this case, one has $d\tilde{\tau}_2/d\tilde{t} = 0$ in equation (38); thus, one can write the luminosity as,

$$\begin{aligned} \tilde{L}^I &= -\frac{(\gamma_{ws} - \gamma_1)}{\gamma_1} \left(\frac{\beta_{ws0}}{\beta_1} - 1 \right) - \frac{m_{ws}}{\dot{m}_1 \gamma_1 \Delta\tau} \frac{d\gamma_{ws}}{d\tilde{t}} \\ &= \frac{(\beta_{ws} - \beta_1)}{\beta_1} \left[\beta_{ws} (\beta_{ws} - \beta_1) \gamma_{ws}^2 - \frac{(\gamma_{ws} - \gamma_1)}{\gamma_1} \right] \end{aligned} \quad (41)$$

where we used that $d\gamma_{ws}/d\tilde{t} = \beta_{ws}\gamma_{ws}^3 d\beta_{ws}/d\tilde{t}$, and, from

equation (7),

$$\frac{d\beta_{ws}}{d\tilde{t}} = -\frac{\dot{m}_1\gamma_1\Delta\tau}{m_{ws}\gamma_{ws}} \frac{(\beta_1 - \beta_{ws})^2}{\beta_1}. \quad (42)$$

On the other hand, in Case II, once the slow material has been completely incorporated at \tilde{t}_c^{II} given by equation (26), $d\tilde{\tau}_1/d\tilde{t} = 0$, and the luminosity is given by

$$\begin{aligned} \tilde{L}^{II} &= \lambda^2 \frac{(\gamma_2 - \gamma_{ws0})}{\gamma_2} \left(a - \frac{\beta_{ws0}}{\beta_1} \right) - \frac{m_{ws}}{\dot{m}_1\gamma_1\Delta\tau} \frac{d\gamma_{ws}}{d\tilde{t}} \\ &= \lambda^2 a \frac{(\beta_2 - \beta_{ws})}{\beta_2} \times \\ &\quad \left[-\beta_{ws}(\beta_2 - \beta_{ws})\gamma_{ws}^2 + \frac{(\gamma_2 - \gamma_{ws})}{\gamma_2} \right], \end{aligned} \quad (43)$$

where, from equation (7),

$$\frac{d\beta_{ws}}{d\tilde{t}} = \frac{\dot{m}_2\gamma_2\Delta\tau}{m_{ws}\gamma_{ws}} \frac{(\beta_2 - \beta_{ws})^2}{\beta_2}. \quad (44)$$

In the ultra-relativistic (UR) limit, $\gamma \gg 1$, the expressions for the luminosities are simplified as shown in Appendix B. In the following section we will apply these equations for the GRB luminosities to describe the light curves of two observed sources.

5 PREDICTED FLUXES

Figure 4 shows the model luminosity for Case I and Case II, normalized to the luminosity in the constant velocity phase, $L^{I,II}/L^0$, as a function of normalized time, $t/t_c^{I,II}$. The models have $\gamma_1 = 100$, $\gamma_2 = 200$, that correspond to the UR limit. Also, we choose $\lambda \sim (br)^{1/2} = 1$, that implies a constant energy injection rate $\dot{m}_1\gamma_1 = \dot{m}_2\gamma_2$. In this case, the critical times (eqs. [14] and [26]) are equal. For this reason, we drop the superscripts in the following discussion. As discussed above, for $t < t_c$, the WS is bounded by 2 shocks and moves at a constant speed. Then, the relative velocity between the incorporated material and the WS and, therefore, the luminosity are constant. For $t \geq t_c$, in both cases one shock disappears and the relative velocities between the WS and the new material that is incorporated decreases with time; therefore, the luminosity, diminishes with time.

Appendix C and D show that, in the UR approximation, one can fit a power-law to the wing of the GRB light curve, and obtain the critical time function \mathcal{T}_c , the gamma ratio, $r = \gamma_2/\gamma_1$, and the mass-loss rate ratio, $b = \dot{m}_2/\dot{m}_1$. These quantities can be obtained without any further assumptions. As an example, Figure 5 shows a model fit to the observed sources GRB 08413B and GRB 070318. The fluxes were taken from Mendoza et al. (2009) that correspond to observations between 15 and 150 keV with the Burst Alert Telescope on board the SWIFT satellite. We first fit the observed flux density F directly and later discuss its relation to the distance and luminosity of the GRB. We follow the procedure described in Appendix D, and choose the value of the luminosity (or flux density) in the constant velocity phase, the time t_0 of the beginning of the velocity pulse, and time $t_e = t_c + t_0$ of the end of the constant velocity phase, where t_c is the critical time of the model. We also choose the flux at the constant velocity phase, F^0 . The wing light curve is then fit by a power-law $F = B(t - t_0)^\alpha$. As discussed in

the Appendix C, the value of the slope α , determines which case (I or II) applies.

Table 1 shows the model parameters that fit the light curves of both GRBs. The name of the GRB is indicated in column 1; the applied model (Case I or Case II) is shown in column 2; column 3 shows the flux in the constant velocity phase; column 4 and column 5 show the time of the beginning of the pulse, t_0 , and the time of the end of the constant velocity phase, t_e ; column 6 and column 7 show the coefficient, B and the exponent α of the power-law fit of the GRB light curve wing; column 8 gives the inferred value of the critical time function, \mathcal{T}_c ; column 9 gives the jump of the flux (or luminosity) at the end of the constant velocity phase, $J(t_e)$ defined by equations (B9) and (B10); finally, column 10 and column 11 give the inferred values of the gamma ratio, r and the mass-loss rate ratio, b , obtained directly from the fit to the wind of the light curve.

In our model, the WS approaches the observer at relativistic speeds. As discussed in Appendix E, the observed bolometric flux density of an approaching relativistic jet is increased with respect to an emitter at rest by a factor δ_{ws}^4 , where $\delta_{ws} = 1/[\gamma_{ws}(1 - \beta_{ws} \cos \theta)]$ and θ is the angle between the direction of the relativistic jet and the observer. Lind & Blandford (1985) obtained an amplification by a factor of δ_{ws}^3 between the observed flux at frequency ν and the emitted luminosity at frequency $\nu' = \nu/\delta_{ws}$. An extra factor of δ_{ws} is obtained when one integrates the frequency to get the observed bolometric flux (or the observed flux in a frequency range) in terms of the emitted bolometric luminosity. Thus, in our model the observed gamma ray flux in the constant velocity phase is given by $F_{GRB}^0 = \delta_{ws0}^4 \tilde{L}_{UR}^0 \epsilon c^2 \gamma_1 \dot{m}_1 / 4\pi D^2$, where \tilde{L}_{UR}^0 is the normalized luminosity in equation (B5).

In order to solve for the mass-loss rate, we assume that the relativistic jet is seen almost along the jet axis, i.e., $\cos \theta \sim 1$, thus, $\delta_{ws0} \sim 2\gamma_{ws0}$. Also, assuming $\gamma_1 = 100$, both \tilde{L}_{UR}^0 and the Lorentz factor γ_{ws0} can be obtained from the model parameters in Table 1. In particular, we obtain large Lorentz factors for the WS, $\gamma_{ws0} \sim 802$ for GRB 080413B, and $\gamma_{ws0} \sim 120$ for GRB 070318 from equation (B2). Furthermore, we estimate the distance to the GRBs from their redshift. The source GRB 070318 has an estimated redshift $z = 0.836$ (Jaunsen et al. 2007) and GRB 080413B has a redshift $z = 1.1$ (Vreeswijk et al. 2008). Assuming a dark energy density $\Omega_\Lambda = 0.7$, a matter density $\Omega_m = 0.3$, and a Hubble constant $H = 70 \text{ km s}^{-1} \text{ Mpc}^{-1}$, the luminosity distance of GRB 070318 is $D = 5300 \text{ Mpc}$ and of GRB 080413B is $D = 7440 \text{ Mpc}$. With all these ingredients, we can now solve for the mass-loss rate, and obtain $\dot{m}_1 \sim 9.7 \times 10^{-6} M_\odot \text{ yr}^{-1}$ for GRB 080413B, and $\dot{m}_1 \sim 1.4 M_\odot \text{ yr}^{-1}$ for GRB 070318. Because the emitting WS moves with relativistic speed, the jet mass-loss rates \dot{m}_1 required to produce the gamma ray flux observed at the Earth are much smaller than those obtained, for example, in nucleosynthesis models of wind-driven supernovae and collapsar models (e.g., Fujimoto et al. 2008; Maeda & Toming 2009).

Note that in the model the time is measured in the frame of reference of the jet source, where the evolution timescales for the WS are of the order of $\sim 10^5 - 10^6 \text{ s}$. Instead, the time of the observations is measured at the observer's frame of reference and is only of the order of tens of seconds if the relativistic jet is seen almost along the jet axis. This happens because the arrival time is $\Delta t_a =$

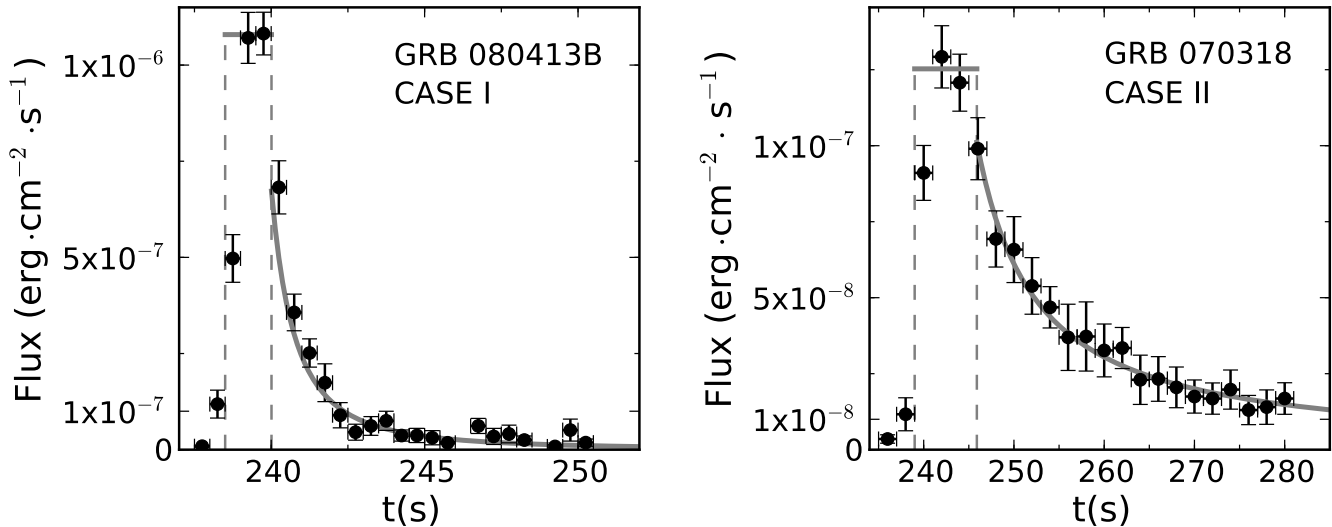


Figure 5. Left panel: GRB 080413B source with a decelerating WS model (thick solid line). Right panel: GRB 070318 source with an accelerating WS model (thick solid line). The thin lines in each panel show the duration of the constant velocity phase. The observational data of both sources was taken from Mendoza et al. (2009).

Table 1. Model Parameters

GRB	Case	F_{GRB}^0 ^a erg cm ⁻² s ⁻¹	t_0 (s)	t_e (s)	$B \pm \Delta B$ (10 ⁻⁷ erg cm ⁻² s ^{-1-α)}	$\alpha \pm \Delta\alpha$	\mathcal{T}_c	J	r ($\frac{\gamma_2}{\gamma_1}$)	b ($\frac{\dot{m}_2}{\dot{m}_1}$)
080413B	I	1.08×10^{-6}	238.50	240.01	15.49 ± 3.00	-2.03 ± 0.30	2.57	0.38	22.49	233.73
070318	II	1.25×10^{-7}	239.00	245.90	8.08 ± 0.50	-1.08 ± 0.05	5.35	0.20	2.64	0.12

^a Flux density in the constant velocity phase, $F_{GRB}^0 = \delta^4 \tilde{L}_{UR}^0 \epsilon c^2 \gamma_1 \dot{m}_1 / 4\pi D^2$.

$\Delta t_{em} / (\gamma_{ws} \delta_{ws})$, where Δt_{em} is the emission time at the jet source frame (e.g., Daigne & Mochkovitch 1998). Also, our models are not meant to explain the shape variation of the bursts with spectral band (e.g., Norris et al. 1996), which would depend on fraction of energy radiated in gamma rays, ϵ . In fact, one expects that ϵ will depend on energy and time, as the WS decelerates and the energy is radiated at lower spectral bands.

Finally, the model uses the simplest velocity variation which allows an analytic solution: it assumes an instantaneous jump in the velocity of the injected material (step function), thus, it makes the simplification that the luminosity instantly achieves the maximum value. A more realistic situation would be a gradual increase in the velocity of the injected material which would produce a gradual growth in the luminosity. Here we show that the decay of two GRB light curves can be fitted by the emission of an decelerated or accelerated WS given by these very simple models. Although, this choice is intended to illustrate the formalism it is also true that the analytic solutions allow an exploration of parameter space and give us an understanding of the dependance of the GRB emission on important physical parameters like the gamma ratio r and the mass-loss rate ratio b .

6 FRACTION OF THE INJECTED MASS LOST BY RADIATION IN THE WS

In this section, we evaluate the fraction of the mass lost by radiation with respect to the mass injected in the WS, Δm . From equation (5) the total mass lost by radiation is

$$\int_0^t L_r(t) c^{-2} dt = \int_{\tau_1}^{\tau_2} \dot{m}(\tau) \gamma(\tau) d\tau - m_{ws}(t) \gamma_{ws}(t). \quad (45)$$

In the RHS of this equation, the first term is the total mass ejected by the flow that has been incorporated into the WS and the second term is the actual mass of the WS. These two terms increase with time but their difference remains finite because the shocks will weaken with time.

One can define the fraction of mass lost by radiation as

$$\Delta m = \frac{\int_0^t L_r(t) c^{-2} dt}{\int_{\tau_1}^{\tau_2} \dot{m}(\tau) \gamma(\tau) d\tau} = 1 - \frac{m_{ws} \gamma_{ws}}{\int_{\tau_1}^{\tau_2} \dot{m}(\tau) \gamma(\tau) d\tau}. \quad (46)$$

This fraction $\Delta m \rightarrow 0$ when $t \rightarrow \infty$ because the total mass lost by radiation in the LHS of equation (45) is finite. Thus, one has to evaluate Δm at a finite time to determine the importance of radiation losses in the dynamics of the working surface.

The total momentum lost by radiation $\int_0^t L_r(t) c^{-2} \beta_{ws} dt$ can be obtained from equation (6). In particular, in the UR regime where $\beta_{ws} \sim 1$, the mass and momentum losses are

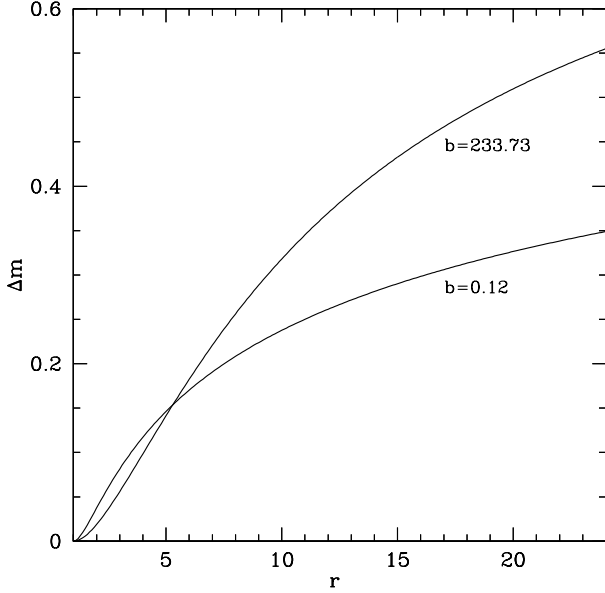


Figure 6. Fraction of mass lost by radiation as a function of the gamma ratio $r = \gamma_2/\gamma_1$. Each curve is labeled by the different values of the mass-loss rate ratio $b = \dot{m}_2/\dot{m}_1$.

the same. In this regime, Δm measures the importance of both momentum and mass losses.

If $\Delta m \ll 1$, radiation losses will not change the relativistic mass of the WS significantly. Note that in the constant velocity phase, radiation losses, which change the relativistic mass of the WS according to equation (5), do not affect the velocity β_{ws} because the LHS of eq. (7) is zero (since $d\beta_{ws}/dt = 0$). Nevertheless, these losses do change the momentum of the WS at the critical time and the dynamics of the WS in the second decelerating/accelerating phase of Case I and II, respectively.

We choose to evaluate Δm at the critical times (eqs. [14] and [26]), which correspond to the end of the constant velocity phase. For Case I, $\tau_{2c} = \Delta\tau$, thus, $\int_{\tau_{1c}}^{\Delta\tau} \dot{m}(\tau)\gamma(\tau)d\tau = \dot{m}_1\gamma_1\Delta\tau a\lambda(1+\lambda)$; for Case II, $\tau_{1c} = -\Delta\tau$, thus, $\int_{-\Delta\tau}^{\tau_{2c}} \dot{m}(\tau)\gamma(\tau)d\tau = \dot{m}_1\gamma_1\Delta\tau(1+\lambda)$. Then, using equations (16), (28), one can show that in both cases I and II, the mass fraction is

$$\Delta m = 1 - \frac{\gamma_{ws}}{\gamma_1} \frac{(b+a\lambda)}{a\lambda(1+\lambda)}. \quad (47)$$

In the UR regime, where $a \sim 1$, $\lambda \sim (br)^{1/2}$, and γ_{ws} is given by equation (B2), this expression reduces to

$$\Delta m = 1 - \frac{r(b+\lambda)}{\lambda(\lambda+r^2)^{1/2}(1+\lambda)^{1/2}}, \quad (48)$$

which is a function only of the gamma ratio, $r = \gamma_2/\gamma_1$, and the mass-loss rate ratio, $b = \dot{m}_2/\dot{m}_1$.

Figure 6 shows Δm as a function of r for the b values of the models presented in Table 1. One can see that the mass fraction is $\Delta m \sim 7\%$ for the model of GRB 070318, but it reaches values $\Delta m > 50\%$ for the model of GRB 080413B. In the last case, radiation losses clearly affect the dynamics of the WS: mass and momentum are not conserved.

7 CONCLUSIONS

We have developed a new formalism that describes the dynamics of an internal WS in a relativistic jet produced by variations in the source injection velocity. The WS is formed when a fast flow overtakes a previous slower flow. This formalism takes into account that the momentum is not conserved because relativistic mass is lost by radiation, in contrast with non relativistic flows.

Assuming step function variations of the injection velocity and mass-loss rate we find analytic solutions for the WS velocity and luminosity. We consider two cases: when a pulse of fast material reaches the slow downstream wind (Case I); and when a pulse of slow material is pushed by fast upstream wind (Case II). In the initial phase, the WS is bounded by 2 shocks: one shock incorporates the material from the fast (slow) pulse, the other shock incorporates material from the slow (fast) wind. In this phase, the velocity of the WS is constant. When the material from the fast (slow) pulse is completely incorporated into the WS, only one shock remains: in Case I, the WS is decelerated as more mass is added to the shock by the slow downstream wind; in Case II, the WS accelerates, pushed by the fast upstream wind. The WS luminosity in the constant velocity phase is constant, and decreases with time when one of the shocks disappears. To apply these models to observed GRBs we assume that a constant fraction ϵ of this energy is emitted in gamma rays.

In the UR limit, the ratio of the Lorentz factors $r = \gamma_2/\gamma_1$ and the mass-loss rates $b = \dot{m}_2/\dot{m}_1$ of the relativistic flows that collide can be obtained directly by fitting the light curves of GRBs. As an example, we fit the light curves of the GRBs 080413B and 070318 with the Case I and Case II models, respectively. For GRB 080413B we obtain the ratios $\gamma_2/\gamma_1 = 22.5$ and $\dot{m}_2/\dot{m}_1 = 233.7$; for GRB 070318 the fit gives lower ratios, $\gamma_2/\gamma_1 = 2.6$ and $\dot{m}_2/\dot{m}_1 = 0.1$. Since the WS is moving towards the observer at relativistic speeds ($\gamma_{ws0} \sim 100 - 800$), one has to correct the observed gamma ray fluxes for Doppler boosting. Assuming $\gamma_1 = 100$, we estimate mass-loss rates of the jets between $\dot{m}_1 \sim 10^{-5} - 1 M_\odot \text{ yr}^{-1}$. Note that the jet kinetic power is $P_{kin} = \gamma \dot{m} c^2 \sim 10^{44-48} \text{ ergs}^{-1}$. This is much smaller than the associated isotropic luminosity, $L_{iso} = 4\pi D^2 F_{GRB}/\epsilon \sim 10^{53-54} \text{ ergs}^{-1}$, uncorrected for relativistic effects. In fact, the isotropic luminosity has no physical meaning for our relativistic jet models, which are able to produce the Doppler boosted gamma ray flux observed at the Earth.

We also evaluate the fraction of the injected mass lost by radiation. For the model of the source GRB 070318 this fraction is $\sim 7\%$, while for the source GRB 080413B, one finds that more than 50% of the injected mass is lost by radiation. Therefore, in the latter source, radiation losses change significantly the relativistic mass of the WS and affect its dynamics.

The step function variability of the source injection velocity and mass-loss rate is a simple approximation to the real time variability of the injection parameters. Other functional time variations of these parameters can be easily implemented in our formalism by integrating the equations in §3 numerically. Nevertheless, in the UR regime our analytic model is very useful to determine the ratios of important

physical parameters (the gamma ratio and the mass-loss rate ratio) without introducing any further assumptions.

In a future work we will study the high energy emission produced by these internal shocks, in particular, the fraction of energy emitted as gamma rays.

ACKNOWLEDGMENTS

J.C., S.L., M.F., R.F.G., and A.H. were supported by PAPIIT-UNAM IN100412 and IN100511. J. C. was also supported by CONACyT 61547. We thank Jose Ignacio Cabrera for providing us with the observational data and Anabella Araudo for useful suggestions. We also thank an anonymous referee for useful comments that helped to improve the paper.

REFERENCES

- Cantó, J., Raga, A. C., & D'Alessio, P. 2000, *MNRAS*, 313, 656
- Daigne, F., & Mochkovitch, R. 1998, *MNRAS*, 296, 275
- Daigne, F., & Mochkovitch, R. 2000, *A&A*, 358, 1157
- Fujimoto, S.-i., Nishimura, N., & Hashimoto, M.-a. 2008, *ApJ*, 680, 1350
- Gehrels, N., Ramirez-Ruiz, E., & Fox, D. B. 2009, *ARA&A*, 47, 567
- Istomin, Y. N. 2010, *MNRAS*, 408, 1307
- Jaunsen, A. O., Fynbo, J. P. U., Andersen, M. I., & Vreeswijk, P. 2007, *GRB Coordinates Network*, 6216, 1
- Kobayashi, S., Piran, T., & Sari, R. 1997, *ApJ*, 490, 92
- Lind, K. R., & Blandford, R. D. 1985, *ApJ*, 295, 358
- Maeda, K., & Tominaga, N. 2009, *MNRAS*, 394, 1317
- Mendoza, S., Hidalgo, J. C., Olvera, D., & Cabrera, J. I. 2009, *MNRAS*, 395, 1403
- Mészáros, P. 2002, *ARA&A*, 40, 137
- Mochkovitch, R., Maitia, V., & Marques, R. 1995, *Ap&SS*, 231, 441
- Norris, J. P., Nemiroff, R. J., Bonnell, J. T., et al. 1996, *ApJ*, 459, 393
- Piran, T. 2004, *Reviews of Modern Physics*, 76, 1143
- Raga, A. C., Binette, L., Canto, J., & Calvet, N. 1990, *ApJ*, 364, 601
- Rees, M. J. 1978, *Nature*, 275, 516
- Rees, M. J. 1984, *ARA&A*, 22, 471
- Rees, M. J., & Meszaros, P. 1994, *ApJ*, 430, L93
- Rybicki, G. B., & Lightman, A. P. 1979, New York, Wiley-Interscience Publication
- Spada, M., Ghisellini, G., Lazzati, D., & Celotti, A. 2001, *MNRAS*, 325, 1559
- Vreeswijk, P. M., Thoene, C. C., Malesani, D., et al. 2008, *GRB Coordinates Network*, 7601, 1

APPENDIX A: COLLISION OF RELATIVISTIC PARTICLES

We discuss a simple example of an inelastic collision of 3 relativistic particles that shows that when energy is radiated

in a shock, momentum is not conserved because the relativistic mass, that includes the Lorentz factor γ_i of internal motions, is not conserved.

Consider two particles in the laboratory with masses m_k , velocity β_k , momentum $P_k = m_k \gamma_k c \beta_k$, and energy, $E_k = m_k \gamma_k c^2$, for particles $k = 1, 2$. We consider the collision between these two particles, where $\beta_2 > \beta_1$. In the laboratory reference frame the momentum conservation (divided by c) gives,

$$m_1 \gamma_1 \beta_1 + m_2 \gamma_2 \beta_2 = (m_1 + m_2) \gamma_{i12} \gamma_{12} \beta_{12}, \quad (\text{A1})$$

where γ_{i12} is the Lorentz factor that corresponds to internal motions, and γ_{12} corresponds to the bulk motion of the new particle 1-2 with velocity β_{12} . Energy conservation (divided by c^2) gives

$$m_1 \gamma_1 + m_2 \gamma_2 = (m_1 + m_2) \gamma_{i12} \gamma_{12}. \quad (\text{A2})$$

The ratio of these two equations gives the velocity of particle 1-2,

$$\beta_{12} = \frac{m_1 \gamma_1 \beta_1 + m_2 \gamma_2 \beta_2}{m_1 \gamma_1 + m_2 \gamma_2}, \quad (\text{A3})$$

and the Lorentz factor for internal motions is obtained from equation (A2)

$$\gamma_{i12} = \frac{m_1 \gamma_1 + m_2 \gamma_2}{(m_1 + m_2) \gamma_{12}}. \quad (\text{A4})$$

Consider a momentum center reference system where the total momentum is zero. This system moves with respect to the laboratory frame with the speed β_{12} defined by equation (A3). The Lorentz transformation of the energy of the two particles before collision in this primed system gives

$$\begin{aligned} E'_k &= \gamma_{12} (m_k \gamma_k c^2 - c \beta_{12} (m_k \gamma_k c \beta_k)) \\ &= m_k \gamma_k \gamma_{12} (1 - \beta_k \beta_{12}) c^2, \end{aligned} \quad (\text{A5})$$

and the momentum transformation gives

$$P'_k = m_k \gamma_k \gamma_{12} c (\beta_k - \beta_{12}). \quad (\text{A6})$$

Using equation (A3), one can check that $P'_1 + P'_2 = 0$.

In this system, after the collision, the new particle 1-2 will be at rest. Before any radiation is emitted, the initial energy before collision $E'_{initial}$ is conserved; thus, after collision it will become the internal energy of the particle 1-2, $E'_{internal}$,

$$\begin{aligned} E'_{initial} &= E'_1 + E'_2 = \frac{(m_1 \gamma_1 + m_2 \gamma_2) c^2}{\gamma_{12}} \\ &= (m_1 + m_2) \gamma'_{i12} c^2 = E'_{internal}, \end{aligned} \quad (\text{A7})$$

where we used equation (A3) to calculate E' , and γ'_{i12} is associated with the internal motions of particle 1-2 in the momentum center reference system. Solving this equation for γ'_{i12} , one gets

$$\gamma'_{i12} = \frac{m_1 \gamma_1 + m_2 \gamma_2}{(m_1 + m_2) \gamma_{12}} = \gamma_{i12}, \quad (\text{A8})$$

where we used equation (A4); i.e., the Lorentz factor associated with internal motions is the same in both reference systems. Thus, after collision the new particle 1-2 has a larger mass, $(m_1 + m_2) \gamma_{i12}$.

Now, let us assume that the particle 1-2 radiates

isotropically (in the momentum center system) all the available energy, thus, the momentum of particle 1-2 will not change, $P'_{12} = 0$. The maximum energy that can be radiated by particle 1-2 is

$$E'_r = E'_{internal} - E'_0 = \frac{c^2}{\gamma_{12}} [m_1\gamma_1 + m_2\gamma_2 - (m_1 + m_2)\gamma_{12}], \quad (\text{A9})$$

where $E'_0 = (m_1 + m_2)c^2$ is the rest energy of particle 1-2, and we used equation (A7).

In the laboratory reference frame, this particle 1-2 that has radiated all the available energy now has an energy and momentum given by the Lorentz transformations

$$E_0 = \gamma_{12} (E'_0 + c\beta_{12}P'_{12}) = (m_1 + m_2)\gamma_{12}c^2; \quad (\text{A10})$$

$$P_0 = \gamma_{12} \left(P'_{12} + \frac{\beta_{12}}{c} E'_0 \right) = (m_1 + m_2)\gamma_{12}c\beta_{12}. \quad (\text{A11})$$

Comparing these equations with the RHS of equations (A1) and (A2) one can see that after radiation, particle 1-2 has lost energy and momentum.

On the other hand, the velocity of particle 1-2 after radiation in the laboratory reference frame is given by

$$\beta \equiv \frac{cP_0}{E_0} = \beta_{12}. \quad (\text{A12})$$

Comparing with equation (A3) one can see that, after radiating all the available energy, particle 1-2 conserves its velocity.

Now, let us consider the collision of three particles with rest masses m_k and velocities β_k , respectively, for $k = 1, 2, 3$. We want to obtain the velocity of the particle that results from the collision of the three particles.

As discussed above, $\beta_2 > \beta_1$, such that particle 2 will collide with particle 1. The resulting velocity of the combined particle 1-2 and internal Lorentz factor are given by equations (A3) and (A4). Now we consider the collision of particle 1-2 with particle 3 that has $\beta_3 > \beta_{12}$.

If the new particle 1-2 collides with particle 3 before it radiates away energy, the conservation of momentum gives

$$(m_1 + m_2)\gamma_{i12}\gamma_2\beta_{12} + m_3\gamma_3\beta_3 = (m_1 + m_2 + m_3)\gamma_{i123}\gamma_{123}\beta_{123}, \quad (\text{A13})$$

and the conservation of energy gives

$$(m_1 + m_2)\gamma_{i12}\gamma_2 + m_3\gamma_3 = (m_1 + m_2 + m_3)\gamma_{i123}. \quad (\text{A14})$$

In this case, where no energy is radiated before the collision of the 3 particles, the velocity of the new particle 1-2-3 is given by the ratio of equations (A13) and (A14)

$$\begin{aligned} \beta_{123}^{ad} &= \frac{(m_1 + m_2)\gamma_{i12}\gamma_2\beta_{12} + m_3\gamma_3\beta_3}{(m_1 + m_2)\gamma_{i12}\gamma_2 + m_3\gamma_3} \\ &= \frac{m_1\gamma_1\beta_1 + m_2\gamma_2\beta_2 + m_3\gamma_3\beta_3}{m_1\gamma_1 + m_2\gamma_2 + m_3\gamma_3}, \end{aligned} \quad (\text{A15})$$

where we used equation (A1) to obtain the last equality. Note that the RHS of the above equation is also obtained from the conservation of momentum and energy of the collision of the 3 particles. If the new particle 1-2-3 radiates all its internal energy, as shown in equation (A12), it will conserve this velocity.

We now consider the case when particle 1-2 radiates

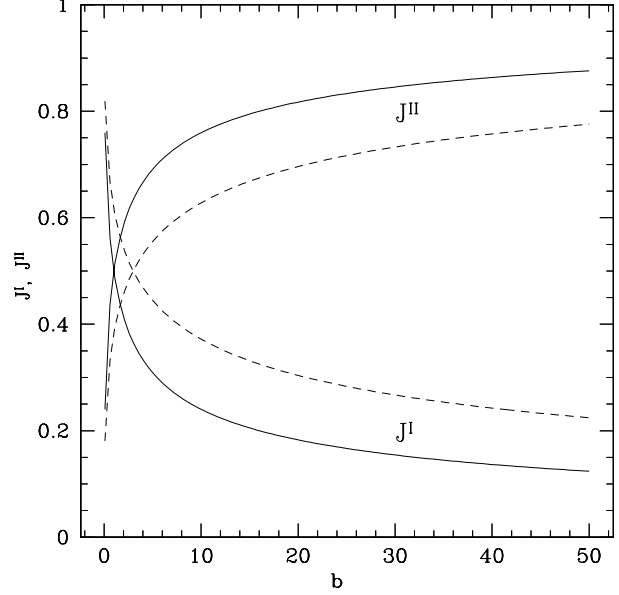


Figure A1. Luminosity jumps J^I and J^{II} as function of the mass-loss rate ratio b for two γ ratios: $r \rightarrow 1$ (solid lines) and $r = 3$ (dashed lines).

all the available energy before colliding with particle 3. In this case, particle 1-2 has the momentum and the energy given by equations (A11) and (A10). Then, the equation of momentum conservation is

$$(m_1 + m_2)\gamma_2\beta_{12} + m_3\gamma_3\beta_3 = (m_1 + m_2 + m_3)\gamma_{i123}\gamma_{123}\beta_{123}, \quad (\text{A16})$$

and the conservation of energy is

$$(m_1 + m_2)\gamma_2 + m_3\gamma_3 = (m_1 + m_2 + m_3)\gamma_{i123}\gamma_{123}. \quad (\text{A17})$$

In this case, when energy is radiated by particle 1-2 before collision with particle 3, the velocity of the new particle 1-2-3 is given by the ratio of equations (A16) and (A17),

$$\beta_{123}^{rad} = \frac{(m_1 + m_2)\gamma_2\beta_{12} + m_3\gamma_3\beta_3}{(m_1 + m_2)\gamma_2 + m_3\gamma_3}. \quad (\text{A18})$$

This velocity is different from the velocity of the adiabatic case, equation (A15). Therefore, the collision of particles that radiate their internal energy does not conserve momentum! This happens because when energy is radiated before collision by particle 1-2 above, its momentum decreases because its relativistic mass $(m_1 + m_2)\gamma_{i12}$ decreases, i.e., $\gamma_{i12} \rightarrow 1$.

Therefore, when energy is radiated in a shock in the collision of 3 relativistic particles, one cannot obtain the velocity of the shock by assuming momentum conservation.

APPENDIX B: THE ULTRA-RELATIVISTIC CASE

Here we will consider the ultra-relativistic (UR) limit, $\beta \simeq 1$, where the Lorentz factor $\gamma \gg 1$. In this limit, $a \sim 1$, and one can expand $\beta \simeq 1 - 1/(2\gamma^2)$. Thus, $\beta_{ws} - \beta_1 \simeq (\gamma_{ws}^2 - \gamma_1^2)/2\gamma_1^2\gamma_{ws}^2$, and $a - 1 \sim (\gamma_2^2 - \gamma_1^2)/(2\gamma_1^2\gamma_2^2)$.

We define the normalized Lorentz factors $r_1 = \gamma_{ws}/\gamma_1$ and $r_2 = \gamma_{ws}/\gamma_2$.

In the constant velocity phase, the velocity of the WS, given by equation (13), can be written as

$$\beta_{ws0} \simeq 1 - \frac{\gamma_2^2 + \lambda\gamma_1^2}{2\gamma_1^2\gamma_2^2(1+\lambda)}, \quad (\text{B1})$$

where $\lambda \sim (br)^{1/2}$ (eq. [12] with $a = 1$). Thus, the constant Lorentz factor is

$$\gamma_{ws0} \simeq \frac{(1+\lambda)^{1/2}\gamma_1\gamma_2}{(\gamma_2^2 + \lambda\gamma_1^2)^{1/2}}, \quad (\text{B2})$$

and the normalized Lorentz factors are constant and are given by

$$r_1^0 = \frac{(1+\lambda)^{1/2}r}{(r^2+\lambda)^{1/2}}, \quad \text{and} \quad r_2^0 = \frac{r_1^0}{r}. \quad (\text{B3})$$

In the decelerating Case I and the accelerating Case II, the normalized Lorentz factors depend on time and are simply given by (eqs. [19] and [31])

$$r_1^I = \frac{\mathcal{T}^I + 2}{\mathcal{T}^I - 2}, \quad \text{and} \quad r_2^{II} = \frac{\mathcal{T}^{II} - 2}{\mathcal{T}^{II} + 2}, \quad (\text{B4})$$

where the time functions $\mathcal{T}^i(\tilde{t})$ are given by equations (23) and (35), respectively.

Thus, the luminosity in the constant velocity phase (eq. [40]) is

$$\begin{aligned} \tilde{L}_{UR}^0 &\simeq \frac{\gamma_{ws0}^2 - \gamma_1^2}{2\gamma_1^2\gamma_{ws0}^2} \left[\lambda \frac{(\gamma_2 - \gamma_{ws0})}{\gamma_2} - \frac{(\gamma_{ws0} - \gamma_1)}{\gamma_1} \right], \\ &\simeq \frac{1}{2\gamma_1^2} \frac{(r_1^0 + 1)(r_1^0 - 1)^2(r_1^0 - r_2^0)}{(r_1^0)^2(1 + r_2^0)}, \end{aligned} \quad (\text{B5})$$

where the last term was obtained by solving for λ in equation (B3). The luminosity of the decelerating Case I (eq. [41]) in the UR case simplifies to

$$\tilde{L}_{UR}^I(\tilde{t}) \simeq \frac{1}{4\gamma_1^2} \frac{(r_1^I + 1)(r_1^I - 1)^3}{(r_1^I)^2} = \frac{32}{\gamma_1^2} \frac{\mathcal{T}^I}{([\mathcal{T}^I]^2 - 4)^2}, \quad (\text{B6})$$

and the luminosity of the accelerating Case II (eq. [43]) simplifies to

$$\begin{aligned} \tilde{L}_{UR}^{II}(\tilde{t}) &\simeq \frac{\lambda^2}{4\gamma_2^2} \frac{(r_2^{II} + 1)(1 - r_2^{II})^3}{(r_2^{II})^2} \\ &= \frac{32\lambda^2}{\gamma_2^2} \frac{\mathcal{T}^{II}}{([\mathcal{T}^{II}]^2 - 4)^2}. \end{aligned} \quad (\text{B7})$$

Finally, the dimensional luminosities are

$$L_{UR}^i = l^i \frac{32\mathcal{T}^i(t)}{([\mathcal{T}^i(t)]^2 - 4)^2}, \quad (\text{B8})$$

where $l^I = \epsilon c^2 \dot{m}_1 / \gamma_1$ for Case I, and $l^{II} = \epsilon c^2 \dot{m}_2 / \gamma_2$ for Case II.

We now examine the ‘‘jump’’ in the luminosity at the critical time t_c^i . At this time, $r_{1,I}$ and $r_{2,II}$ coincide with $r_{1,0}$ and $r_{2,0}$, respectively, given by eqs. (B3), because the velocity of the WS is a continuous function of time. Then, we define the jump of the luminosities at t_c^i as

$$J^I = 1 - \frac{L_{UR}^I(t_c^I)}{L_{UR}^0} = \frac{(r_1^0 + 1)(1 - r_2^0)}{2(r_1^0 - r_2^0)}, \quad (\text{B9})$$

for Case I, and

$$J^{II} = 1 - \frac{L_{UR}^{II}(t_c^{II})}{L_{UR}^0} = \frac{(r_1^0 - 1)(1 + r_2^0)}{2(r_1^0 - r_2^0)}, \quad (\text{B10})$$

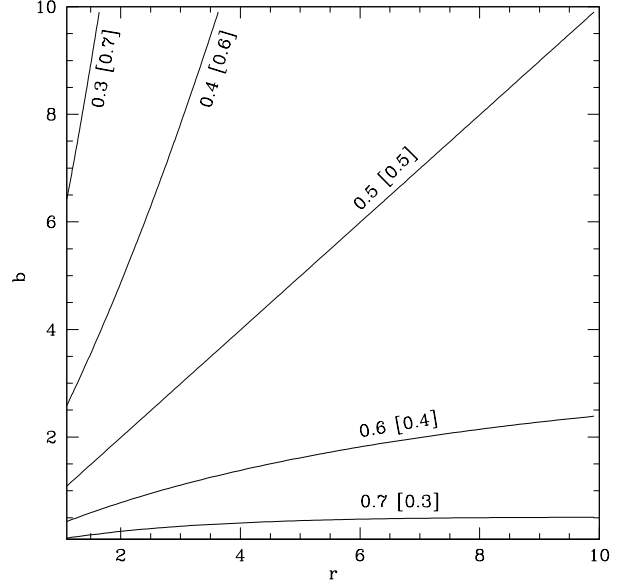


Figure B1. Isocontours of the luminosity jump as function of the mass-loss rate ratio, b , and the gamma ratio, r . Each contour is labeled by the value of the jump for Case I and, in square brackets, the value of the jump for Case II.

Table B1. Coefficients

Case	a_0	a_1	a_2	b_1	b_2
I	-2.0000	-1.6724	-0.3646	0.7635	0.2431
II	-0.6667	-0.5494	-0.2651	0.6247	0.1768

for Case II, where we used equations (B5), (B6), and (B7). The luminosity jumps are shown in Figure A1 as a function of the mass-loss rate ratio b for two values of the gamma ratio r : $r \rightarrow 1$ (solid line) and $r = 3$ (dashed line). One can see that small luminosity jumps are predicted for large values of b in Case I; the opposite is true for Case II. The figure also shows that the summ $J^I + J^{II} = 1$ because at the critical time, the WS of Case I and Case II are each one bounded by only one of the shocks that provide the total luminosity, L^0 , in the constant velocity phase. This fact is also presented in Figure B1 by isocontours of the luminosity jumps J^I and J^{II} as functions of the mass-loss rate ratio b and gamma ratio r .⁷

APPENDIX C: THE CRITICAL TIME FUNCTION, \mathcal{T}_C

This Appendix describes a procedure to obtain the critical time function, \mathcal{T}_c , from a fit of the GRB light curve. Let us assume that the constant velocity phase starts at an observed time t_0 , then, the decaying wing of the GRB light curve starts at $t_e = t_0 + t_c$, where t_c is the critical time (t_e

⁷ It can be shown from equations (11), (40), (41), and (43), that $L^0 = L^I + L^{II}$, is a general result, not only valid for the UR case.

measures the end of the constant velocity phase). We further assume that the wing of the GRB light curve can be fit by a power-law, $L = B(t - t_0)^\alpha$, $t > t_e$. Consider three times: $t_n = nt_c + t_0$, $n = 1, 2, 3$, and the corresponding dimensional luminosities, $L(\mathcal{T}_n(t_n))$, which are given by equation (B8). Then, one can construct the relation

$$n^\alpha = \frac{\mathcal{T}_n (\mathcal{T}_c^2 - 4)^2}{\mathcal{T}_c (\mathcal{T}_n^2 - 4)^2}, \quad (\text{C1})$$

which can be solved for the time function \mathcal{T}_n as

$$\mathcal{T}_n^4 - 8\mathcal{T}_n^2 - \frac{(\mathcal{T}_c^2 - 4)^2}{n^\alpha \mathcal{T}_c} \mathcal{T}_n + 16 = 0, \quad n = 2, 3. \quad (\text{C2})$$

These are two quartic equations for time functions $\mathcal{T}_n(\mathcal{T}_c, \alpha)$.

Equations (23) and (35) give the relation between the time t and \mathcal{T} for Cases I and II, respectively. Let us define $\mu^I(\mathcal{T}) = \mathcal{T}^2/2 + 4\mathcal{T} + 4\ln \mathcal{T}$, for Case I, and $\mu^{II}(\mathcal{T}) = \mathcal{T}^2/2 - 4\mathcal{T} + 4\ln \mathcal{T}$, for Case II. Then, one can construct the relation

$$\mathcal{H}^{I,II} = \mu^{I,II}(\mathcal{T}_3) - 2\mu^{I,II}(\mathcal{T}_2) + \mu^{I,II}(\mathcal{T}_c) = 0. \quad (\text{C3})$$

When one substitutes $\mathcal{T}_n(\mathcal{T}_c, \alpha)$ from equation (C2) in this equation, one obtains a relation $\mathcal{H}^{I,II}(\mathcal{T}_c, \alpha) = 0$. This relation gives two distinct curves for the critical time function $\mathcal{T}_c(\alpha)$ for Case I and II. These curves can be fit by the Padé polynomials

$$\alpha = \frac{a_0 + a_1(\mathcal{T}_c - 2) + a_2(\mathcal{T}_c - 2)^2}{1 + b_1(\mathcal{T}_c - 2) + b_2(\mathcal{T}_c - 2)^2}, \quad (\text{C4})$$

where the coefficients are given in Table 2. These curves are shown in Figure C1. In particular, the values of the exponent α are restricted to the interval $[-2.02662, -3/2]$ for Case I, and $[-3/2, -2/3]$ for Case II. Thus, from the slope α , one can determine to which case corresponds the observed wing of the GRB light curve: Case I (decelerating WS) vs Case II (accelerating WS).

APPENDIX D: DETERMINATION OF FUNDAMENTAL PARAMETERS: GAMMA RATIO AND MASS-LOSS RATE RATIO IN THE ULTRA RELATIVISTIC CASE.

The gamma ratio and mass-loss rate ratio can be obtained by the following procedure.

I) Given the GRB light curve, one chooses the time for the beginning of the velocity pulse, t_0 (this corresponds to $t = 0$ in the models), and the time for the end of the constant velocity phase, $t_e = t_0 + t_c$, where the critical time is t_c .

II) From a numerical fit of the GRB light curve wing, $L = B(t - t_c)^\alpha$, the critical time \mathcal{T}_c for Case I or Case II can be obtained from equation (C3).

III) From the observations, the jump J of the luminosities at t_c , defined by equation (B9) and equation (B10) for Case I and Case II, respectively, are estimated. Also, from these equations, writing the gamma ratio $r = r_1^0/r_2^0$, with $r_1^0 = (\mathcal{T}_c + 2)/(\mathcal{T}_c - 2)$ for Case I and $r_2^0 = (\mathcal{T}_c - 2)/(\mathcal{T}_c + 2)$ for Case II (see eq. [B4]), it can be shown that,

$$r = \frac{(\mathcal{T}_c + 2)[J(\mathcal{T}_c - 2) - \mathcal{T}_c]}{(\mathcal{T}_c - 2)[J(\mathcal{T}_c + 2) - \mathcal{T}_c]}, \quad (\text{D1})$$

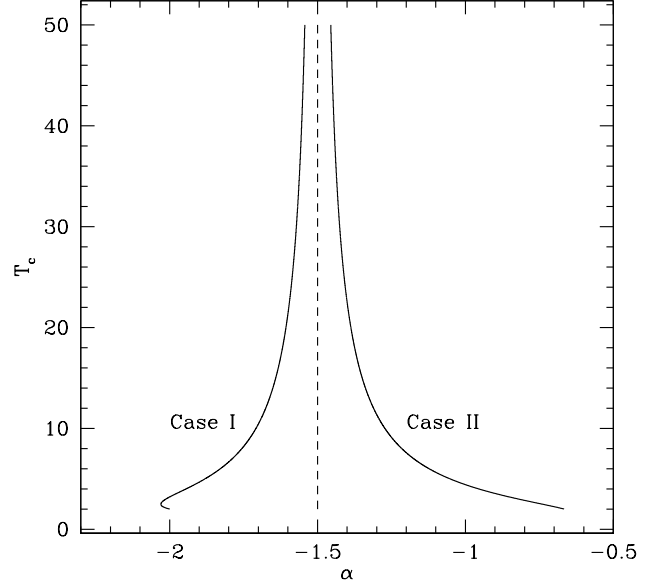


Figure C1. Relation between the exponent α and the critical time, \mathcal{T}_c , for Case I and Case II, obtained from equation (C4).

where this equation applies for both cases I and II.

IV) Finally, the parameter $\lambda = b^{1/2}r^{1/2}$ is calculated from equation (B3), that is,

$$\lambda_I = \frac{[\mathcal{T}_c - J(\mathcal{T}_c - 2)]^2}{J(1 - J)(\mathcal{T}_c - 2)^2}, \quad \text{and} \quad (\text{D2})$$

$$\lambda_{II} = \frac{J(1 - J)(\mathcal{T}_c + 2)^2}{[\mathcal{T}_c - J(\mathcal{T}_c + 2)]^2}. \quad (\text{D3})$$

Therefore, only the ratios λ and r can be obtained independently by fitting the observations in the UR case. Finally, from λ and r one can obtain the mass-loss rate ratio $b = \lambda^2/r$.

APPENDIX E: DOPPLER BOOSTING

As found by Lind and Blandford (1985), for a WS in a relativistic jet approaching the observer with a velocity β_{ws} , the observed flux at a given frequency, F_ν is increased with respect to an emitter at rest by a factor δ_{ws}^3 , where the Doppler factor is $\delta_{\text{ws}} = 1/[\gamma_{\text{ws}}(1 - \beta_{\text{ws}} \cos \theta)]$, where θ is the angle between the observer and the jet axis.

In particular, for an optically thin WS, the observed flux is given by

$$F_\nu = \frac{\delta_{\text{ws}}^3}{D^2} \int_{V'} j'_{\nu'} dV', \quad (\text{E1})$$

where D is the distance to the jet source and $j'_{\nu'}$ is the volume emissivity ($\text{erg cm}^{-3} \text{s}^{-1} \text{str}^{-1} \text{Hz}^{-1}$) at frequency $\nu' = \nu/\delta_{\text{ws}}$ measured in the rest frame of the emitting source, and the integration is carried over the volume V' .

Integrating the flux over a 4π solid angle and over the

frequency ν' , one gets

$$4\pi \int_0^\infty F_\nu d\nu' = \frac{\delta_{\text{ws}}^3}{D^2} 4\pi \int_0^\infty \int_{V'} j'_{\nu'} dV' d\nu'.$$

Given the transformation $\nu' = \nu/\delta_{\text{ws}}$, the integral in the LHS of the above equation is

$$\int_0^\infty F_\nu d\nu' = \frac{1}{\delta_{\text{ws}}} \int_0^\infty F_\nu d\nu, \quad (\text{E2})$$

therefore, the bolometric flux is

$$F_{\text{bol}} \equiv \int_0^\infty F_\nu d\nu = \frac{\delta_{\text{ws}}^4}{4\pi D^2} L', \quad (\text{E3})$$

where L' (erg s^{-1}) is the bolometric luminosity or the total emitted power of the source.

In our model, the luminosity of the WS in equation (38), L_r , is measured in the rest frame of the source of the jet. This total emitted power is a Lorentz invariant for any source that emits isotropically in its instantaneous frame of reference (Rybicki & Lightman 1979). Thus, $L_r = L'$. Furthermore, since we consider that a fraction ϵ of the bolometric luminosity is emitted in gamma rays, $L_{\text{GRB}} = \epsilon L_r$ (see §4), then, the observed flux in gamma rays, $F_{\text{GRB}} = \epsilon F_{\text{bol}}$, is given by

$$F_{\text{GRB}} = \frac{\delta_{\text{ws}}^4}{4\pi D^2} L_{\text{GRB}}. \quad (\text{E4})$$

This equation can also be written in terms of the non dimensional luminosity in equation (39) as

$$F_{\text{GRB}} = \frac{\delta_{\text{ws}}^4}{4\pi D^2} \tilde{L} \epsilon \dot{m}_1 \gamma_1 c^2. \quad (\text{E5})$$

The case of an optically thick WS, discussed by Lind & Blandford (1985), follows in a straight forward fashion. One also obtains the δ_{ws}^4 factor between the emitted and observed bolometric fluxes because the extra δ_{ws} factor is due to the integration in frequency.

This paper has been typeset from a $\text{\TeX}/\text{\LaTeX}$ file prepared by the author.